EARLY-TIME PULSE-ECHO THERMAL WAVE IMAGING

Xiaoyan Han, L.D. Favro, P.K. Kuo and R.L. Thomas
Department of Physics and Institute for Manufacturing Research
Wayne State University, Detroit, MI 48202, USA

INTRODUCTION

We describe the early time behavior of reflected thermal wave pulses from planar subsurface scatterers, and describe methods for making depth images, independently of the lateral size of the scatterer.

THEORY AND EXPERIMENT

The three-dimensional thermal wave diffraction from a subsurface planar scatterer of arbitrary shape, f (x',y'), in a thermally anisotropic material, can be written as

$$T - T_o = \frac{1}{2\pi}\left(\frac{1}{\pi\alpha_1\alpha_2\alpha_3 t}\right)^{1/2} \int_{-\infty}^{\infty}\int_{-\infty}^{\infty} dx'\,dy' \sum_{m=1}^{\infty} \frac{A^m}{R_m}\frac{1}{\alpha_3^{1/2}}\left[\frac{\partial}{\partial z}\exp\left(-\frac{\left[R_m + (z^2/\alpha_3)^{1/2}\right]^2}{4t}\right)\right]_{z=\ell} f(x', y') \quad , \quad (1)$$

where

$$R_m = \left[\frac{(x - x')^2}{\alpha_1} + \frac{(y - y')^2}{\alpha_2} + \frac{(2m-1)^2\,\ell^2}{\alpha_3}\right]^{1/2} ,$$

and where A is the reflection coefficient at a boundary, which can be written in terms of ratios of effusivities of the materials on either side of the boundary. In Eq. (1), α_i are the components of the anisotropic thermal diffusivity of the material, and t is the time after the flash at which the image is acquired. The summation over the index, m, takes into account multiple reflections of the thermal wave pulse between the subsurface scatterer and the surface of the material. Such reflections are increasingly important when the lateral dimensions of the subsurface scatterer become large, or when the scatterer is close to the surface.

Figure 1 shows schematic diagrams of two flat-bottomed hole specimens used to test the predictions of Eq. (1). One of the specimens has six holes milled into the rear surface of the sample. The flat bottoms of these holes are 1 - 5 mm beneath the painted front surface. The other specimen has five milled holes of diameters ranging from 6 mm to 50 mm, all located at the same depth, 1.2 mm. Figure 2 is a schematic representation of the predictions of Eq. 1, and indicates two characteristic features, the peak contrast time and the peak slope time, which we have used to produce both theoretical and experimental images of the samples shown in Fig. 1. The purpose of using these features is to study their reliability for measuring the depths of such holes, independently of their lateral sizes.

Review of Progress in Quantitative Nondestructive Evaluation, Vol. 15
Edited by D.O. Thompson and D.E. Chimenti, Plenum Press, New York, 1996

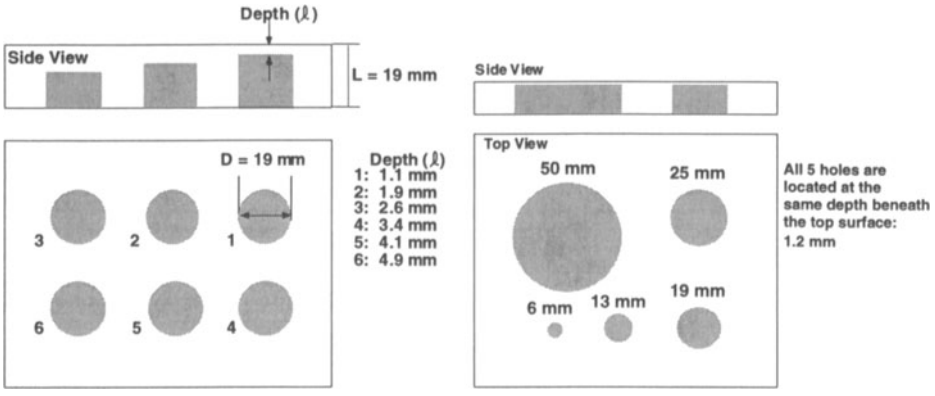

Fig. 1 Schematic diagram of two flat-bottomed hole specimens used to test the predictions of Eq. (1).

Using Eq. (1), we calculate the peak contrast time (see Fig. 2) at every point on the surfaces of the two samples shown schematically in Fig. 1. Then, instead of forming an image from the actual contrast data, we use the peak contrast times themselves.. Since, as will be shown below, the peak contrast times depend upon the depths of the holes, such images have in the past been interpreted as being depth images, where the time is a linear function of the square of the depth. Our six-hole sample has been used to illustrate the dependence of the peak contrast on depth. In Fig. 3, we show a theoretical peak contrast time image, together with the corresponding experimental peak contrast time image of the actual six-hole sample. The plots below these two images in Fig. 3 show the peak contrast times just above the centers of the holes as a function of the square of the depths. The theoretical plot is a straight line, with a non-zero intercept on the time axis. The data in the experimental image were intended to illustrate the short-time behavior of the thermal wave, and therefore the experiment was not run long enough to obtain peak contrast times on more than the two shallowest holes. However, these two points are in semi-quantitative agreement with the theoretical plot. The small quantitative difference is believed to be due

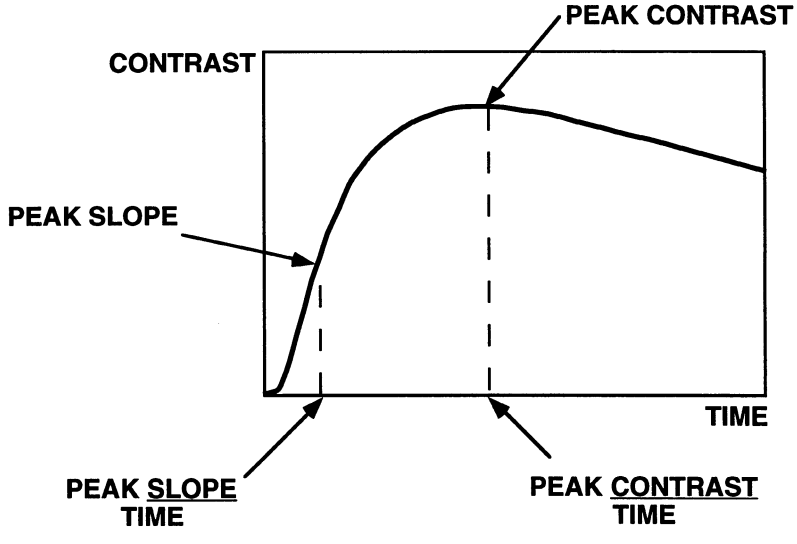

Fig. 2 Sketch of a typical thermal wave contrast curve (the surface temperature over the defect minus the surface temperature over a background region) as a function of time. The times indicated are possible candidates for making depth measurements.

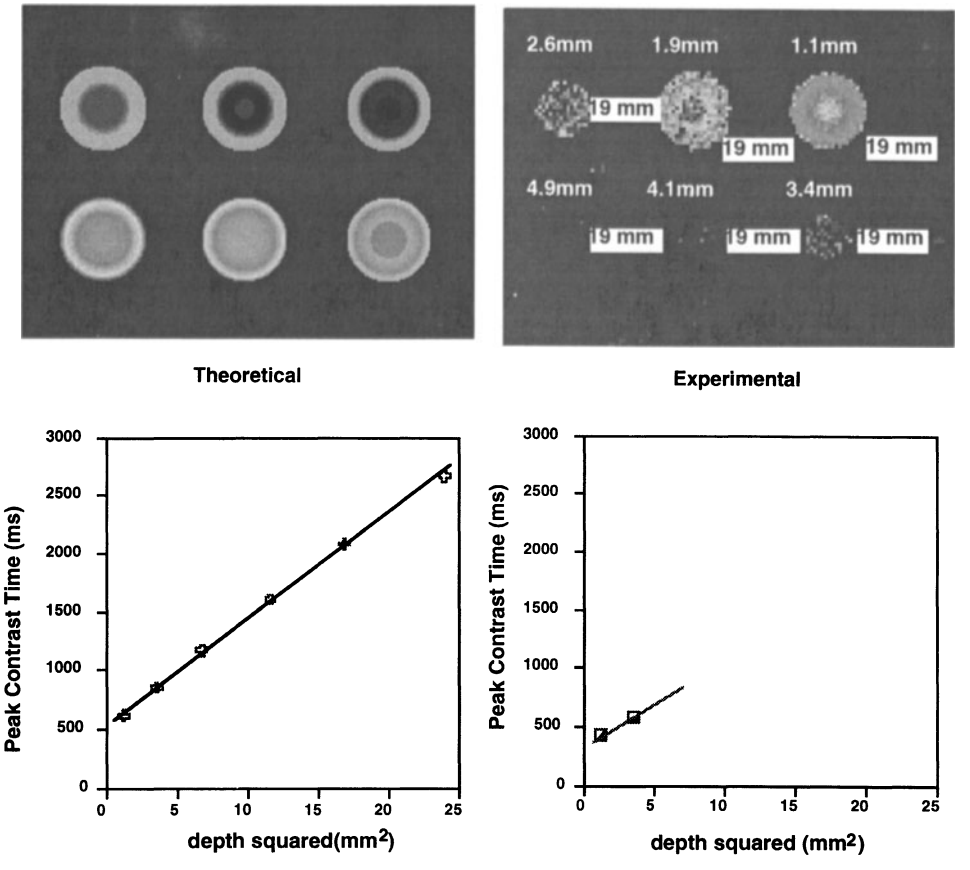

Fig. 3 Theoretical and experimental images (top left and right, respectively) of the peak contrast times for the six-hole sample shown schematically in Fig. 1. The two corresponding plots below these two images show the depth-dependence of the peak contrast time above the centers of the holes.

to an incorrect choice of the thermal diffusivity in theoretical calculation. The fact that the intercepts of both of these plots are non-zero results from the effects of multiple thermal wave reflections of the thermal wave pulse between the top of the hole and the sample surface. These effects are more important for the shallower holes and therefore lift the low end of the curve. The physical effect arises from the fact that thermal wave pulses broaden dramatically as they get further away from the source, so that successive reflected pulses (echoes) overlap each other in time, with the result that the peak of the contrast curve shown in Fig. 1 is shifted towards longer time by the reflections which arrive later. Since the shallowest holes produce more reflections, they experience a greater shift. The results presented in Fig. 3 would appear to indicate that with proper calibration, one could use the peak contrast time to measure the depths of defects in a sample. However, the second test specimen, which has five flat-bottomed holes, all at the same depth, but with widely varying diameters will be used below to demonstrate that the peak contrast time depends not only on the depth but also on the lateral size of the defect.

In Fig. 4, we show the results of a comparison of theory and experiment similar to that described above, but for the second test sample, containing five holes at constant depth. The plots below the two images of Fig. 4 show clearly that the peak contrast times increase dramatically with the diameter of the holes. In fact, experimentally, the largest (50 mm) hole had not yet reached its peak contrast in the time allocated for the experiment. Its indicated peak contrast time was the length of time over which the images were obtained,

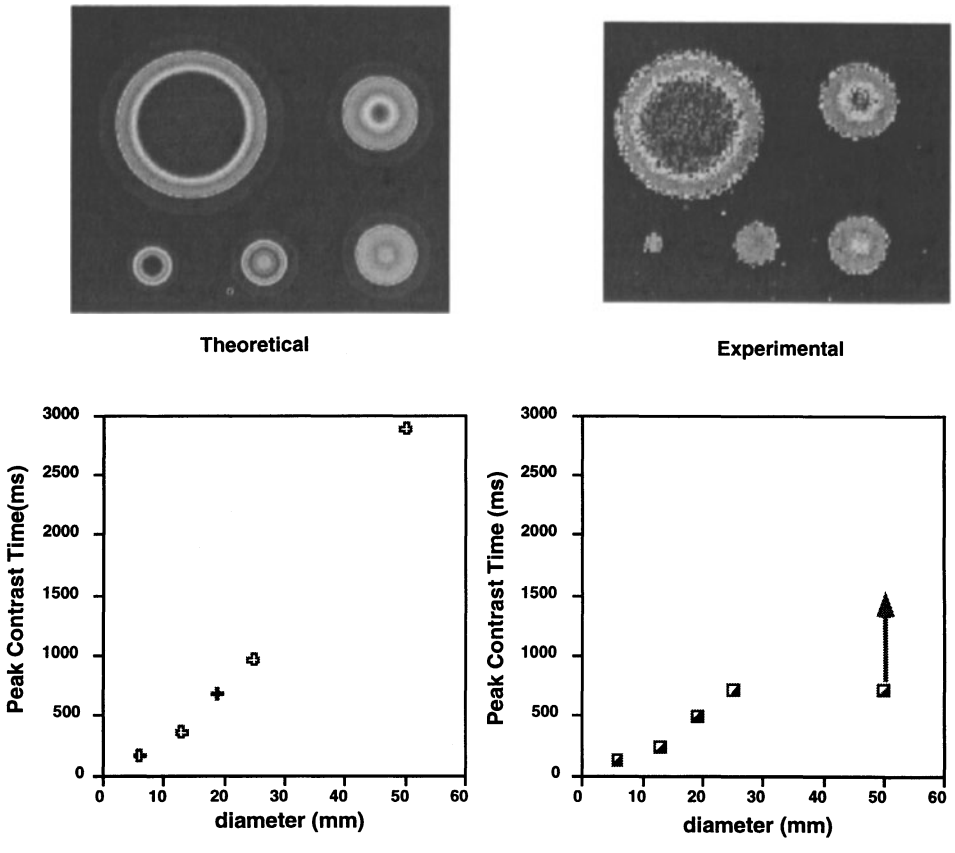

Fig. 4 Theoretical and experimental images (top left and right, respectively) of the peak contrast times for the five-hole sample shown schematically in Fig. 1. The two corresponding plots below these two images show the diameter-dependence of the peak contrast time above the centers of the holes.

and the arrow is attached to indicate that the actual peak contrast time for this largest hole is considerably longer. This effect is also due to multiple reflections. The larger the diameter of the hole, the longer the pulses can reflect back and forth between the surfaces before they leak out around the edges. Again, the overlapping of the broad echo pulses causes the peak contrast to be shifted to longer times for the larger holes.

The inability of the peak contrast time to discriminate the depth of a defect independently of its size leads one to look for some other feature of the contrast curve which might be used to measure the depth. Since leading edge of the contrast curve should be almost totally dominated from the first pulse which returns from the defect, a suitable choice for such a feature is the peak slope time, shown schematically in Fig. 2. A test of its dependence upon the depth of the defect is shown in Fig. 5, for the six-hole sample. The plots below the two images of Fig. 5 show clearly that the peak slope times increase in proportion to the square of the diameter of the holes. However, unlike the corresponding plots for the peak contrast time (compare Fig. 3), these plots extrapolate through the origin, indicating a strict quadratic dependence between this characteristic thermal pulse transit time and the depth of the reflector. To confirm this relationship, in Fig. 6 we test the independence of the peak slope time on the lateral size at constant depth, once again using the five-hole test sample. It can be seen from the theoretical and experimental images, and the corresponding plots of their peak slope times as a function of the hole diameter, that multiple reflections, and hence lateral defect sizes, make an insignificant contribution to this characteristic early-time feature of the thermal wave contrast curve.

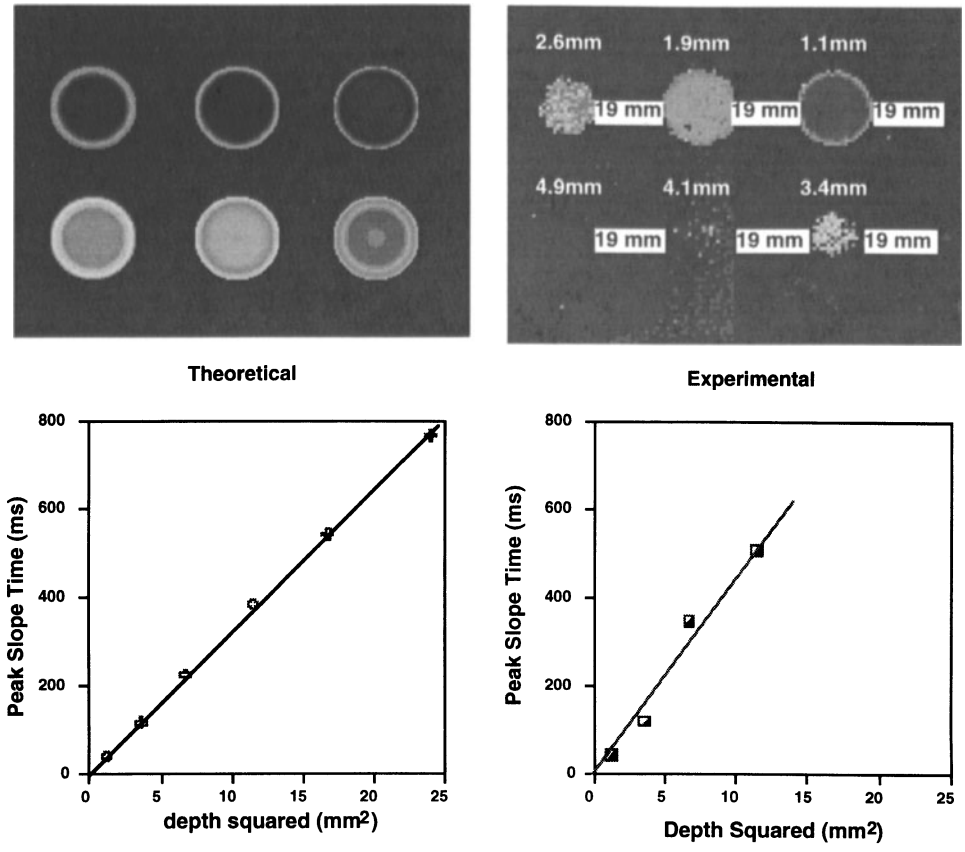

Fig. 5 Theoretical and experimental images (top left and right, respectively) of the peak slope times for the six-hole sample shown schematically in Fig. 1. The two corresponding plots below these two images show the depth-dependence of the peak slope time above the centers of the holes. The experimental data did not extend long enough in time to resolve the deepest two holes. The slight difference between the predicted and observed slopes of the two curves can be accounted for by the uncertainty in the assumed thermal diffusivity for the steel sample (0.136 cm^2/s).

CONCLUSIONS

We have shown that three-dimensional thermal wave diffraction and multiple reflection calculations accurately describe the pulse-echo imaging of circular, planar subsurface defects. Whereas utilization of the peak contrast time for defect depth determination is complicated by its dependence on the contributions from multiple reflections, the earlier, peak slope, time of the same curve has been shown to have minimal contributions from multiple reflections, and hence is essentially independent of the lateral size of the defect. Finite element modeling calculations by other workers [1,2] have recently come to the same general conclusions.

ACKNOWLEDGMENTS

This work is sponsored by the FAA-Center for Aviation Systems Reliability, operated at Iowa State University and supported by the Federal Aviation Administration Technical Center in Atlantic City, New Jersey, under grant number 94-G-011, by AFOSR, under Grant No. F49620-93-1-0428, and by the Institute for Manufacturing Research.

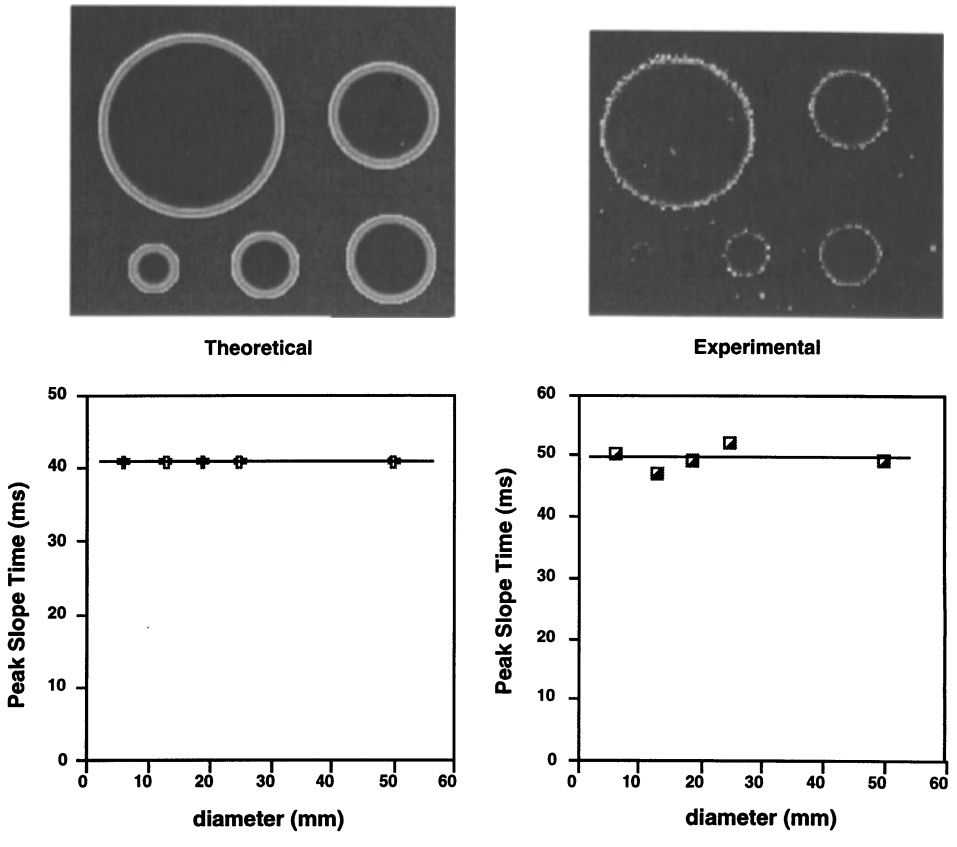

Fig. 6 Theoretical and experimental images (top left and right, respectively) of the peak slope times for the five-hole sample shown schematically in Fig. 1. The two corresponding plots below these two images show the diameter-dependence of the peak slope time above the centers of the holes.

REFERENCES

1. H.I. Ringermacher, Abstract for the Rev. Prog. QNDE, July 30 - Aug. 4, 1995, Seattle, WA, p. 132.
2. S. Saintey and D.P. Almond, Abstract for the Rev. Prog. QNDE, July 30 - Aug. 4, 1995, Seattle, WA, p. 133.